Supporting Information

NanoRNP Overcomes Tumor Heterogeneity in Cancer Treatment

Qi Liu[†], Jinquan Cai[§], Yadan Zheng[†], Yanli Tan[#], Yunfei Wang[‡], Zhanzhan Zhang[†], Chunxiong Zheng[†], Yu Zhao[†], Chaoyong Liu[‡], Yingli An[†], Chuanlu Jiang[§], Linqi Shi*[†], Chunsheng Kang*[‡], and Yang Liu*[†]*

[†] State Key Laboratory of Medicinal Chemical Biology, Key Laboratory of Functional Polymer Materials of Ministry of Education, College of Chemistry, Nankai University, Tianjin, 300071, China.

[‡]Laboratory of Neuro-Oncology, Tianjin Neurological Institute, Department of Neurosurgery, Tianjin Medical University General Hospital, Key Laboratory of Neurotrauma, Variation, and Regeneration Ministry of Education and Tianjin Municipal Government, Tianjin, 300052, China.

[§]Neuroscience Institute Department of Neurosurgery, The Second Affiliated Hospital of Harbin Medical University, Heilongjiang Academy of Medical Sciences, Harbin 150086, China.

[#]Department of Pathology, Affiliated hospital of Hebei University, Baoding 071000, China.

*E-mail: jcl6688@163.com, *E-mail: shilinqi@nankai.edu.cn, *E-mail: kang97061@tmu.edu.cn, *E-mail: yliu@nankai.edu.cn

*[†]Tel.: 0086-22-83662812; Fax: 0086-22-23503510.

Materials and methods

Materials. Reagents and solvents were purchased from Sigma-Aldrich (Shanghai, china) and used as received without further purification unless otherwise noted. Dialysis membranes were purchased from Tian Nan Science and Technology (Tianjin, China). Malignant glioma cell line (U87MG) were purchased from American Type Culture Collection (ATCC). Cas9 nuclease was purchased from New England Biolabs (UK). The Dulbecco's Modified Eagle Medium (DMEM) growth medium, fetal bovine serum (FBS), 0.05% trypsin, and penicillin/streptomycin were purchased from Gibco (Thermo Fisher, USA). FITC, paraformaldehyde, and 4,6-diamidino-2-phenylindole dihydrochloride (DAPI) were purchased from Invitrogen (USA). Cy5-NHS and Cy3-NHS were obtained from Oukainasi Technology (Beijing, China). AmpliScribe™ T7-Flash™ Transcription Kit and T7 Endonuclease I Kit was obtained from Epicentre. Bicinchoninic acid (BCA) protein assay kit was obtained from Solarbio Science & Technology (Beijing, China). Cell genomic DNA extraction kit and DNA purification kit were purchased from TIANGEN Biotech (Beijing, China). Cell Counting Kit-8 (CCK-8) was obtained from Zhuangmeng Biotech (Beijing, China). Fluorescent TUNEL staining kit was obtained from Zhongshanjinqiao Biotech (Beijing, China). ABC-peroxidase, diaminobenzidine (DAB) were purchased from Bersin Biotech (Guangzhou, China). Hairpin-it miRNA qPCR Quantitation Kit was obtained from GenePharma Biotech (Shanghai, China). All ELISA kits was purchase from Elabscience Biotechnology Co., Ltd (Wuhan, China). All the antibodies were purchased from Santa Cruz Biotech (Shanghai, China).

Synthesis of $PLys_{100}$. The $PLys_{100}$ was synthesized by the ring-opening polymerization of Lys(Z)-NCA using butylamine as the initiator.[1] Briefly, Lys(Z)-NCA (4.28 g, 14.72 mmol) was dissolved

in 30 mL of N,N-Dimethylformamide (DMF). Polymerization was initiated by the addition of butylamine (0.009 g, 0.123 mmol). The reaction mixture was stirred for 3 days at 35°C under a dry argon atmosphere. After the reaction, the solvent was evaporated under reduced pressure. The resulting product was dissolved in 15 mL of $CHCl_3$ and then precipitated into excessive diethyl ether to obtain PLys(Z) (yield 80%). Deprotection of Z group in PLys(Z) was carried out by addition of HBr (33 wt.% in HOAc, 2 mL) to the solution of PLys(Z) (2.0 g) in 20 mL CF_3COOH for 2 h at 0°C. After precipitating using cold diethyl ether, the product was re-dissolved in DMF and filtered through a 0.22 μm Millipore filter. The filtrate was precipitated in excessive diethyl ether to remove the residual CF_3COOH and obtain PLys (yield 65%). PLys was characterized using ^{1}H NMR. As shown in Figure S2, the degree of polymerization (DP) of Lys was estimated to be 100 by comparing the integration of the peaks of the $CH_3CH_2CH_2CH_2$- protons of butylamine at 3.3-3.4 ppm and the -NHCHCO- protons of $PLys_{100}$ at 4.2-4.4 ppm. ^{1}H NMR (400 MHz, D_2O, δ ppm): δ=4.2-4.4: (1H, -NHCHCO-), δ=2.8-3.1: (2H, -CH_2NH_2), δ=1.2-1.8: (6H, -$CH_2CH_2CH_2CH_2NH_2$).

Synthesis of $mPEG_{77}$-CA. The synthesis of $mPEG_{77}$-CA was achieved by modifying $mPEG_{77}$-OH (MW: 3400) with 2,5-dihydro-2,5-dioxofuran-3-acetic acid (CA) (Figure S1). Briefly, CA (0.276 g, 1.5 mmol) was dissolved in 10 mL dry dichloromethane, and then oxalyl chloride (0.378 g, 3mmol) was added at 0°C, DMF (40 μL) were added as catalyst. The solution was stirred for 15 minutes, and then transferred to 25°C for further reaction for 1 h. After the reaction, the solution was dried by rotary evaporation, the chlorine-substituted CA was then reacted with $mPEG_{77}$-OH (1.7 g, 0.5 mmol) in 5 mL dry dichloromethane with 30 μL of pyridine as the catalyst. The reaction was performed at 25°C for 3 h and terminated by adding an equal volume of saturated ammonium chloride aqueous solution. The organic phase was separated, collected, dried and precipitated into

anhydrous diethyl ether at 0°C twice. The obtained product was dried to produce a brown powder with a yield of 91%. The $mPEG_{77}$-CA was characterized using ^1H NMR.[2, 3] As shown in Figure S2, ^1H NMR (400 MHz, D_2O, δ ppm): δ=6.3-6.4: (1H, $-CH_2C(CO)CHCO-$), δ=3.5-3.7: (4H, $-CH_2CH_2O-$), δ=3.5-3.7: (2H, $-OCCH_2C(CH)CO-$), δ=3.2-3.4: (3H, CH_3O-).

Synthesis of $PLys_{100}$-CA-$mPEG_{77}$. The synthesis of $PLys_{100}$-CA-$mPEG_{77}$ was achieved by conjugating $mPEG_{77}$-CA with $PLys_{100}$ (Figure S1). Briefly, 100 mg $PLys_{100}$ was dissolvedd in sodium bicarbonate buffer (pH 8.5, 50 mM) to reach a concentration of 10 mg/mL, and then 221.2 mg of $mPEG_{77}$-CA (eight equivalents to $PLys_{100}$) were added. During the reaction, the pH of the solution was maintained in the range of 8.0-8.5 using 0.2 N NaOH. After the reaction, unreacted $mPEG_{77}$-CA was removed by dialysis (MWCO=10000 Da), and $PLys_{100}$-CA-$mPEG_{77}$ was obtained by lyophilization. The successful synthesis was confirmed using ^1H NMR analysis (Figure S2). ^1H NMR (400 MHz, D_2O, δ ppm): δ=4.2-4.4: (1H, $-NHCHCO-$),δ=3.5-3.7: (4H, $-CH_2CH_2O-$), δ=3.5-3.7: (2H, $-OCCH_2C(CH)CO-$), δ=2.8-3.1: (2H, $-CH_2NH_2$), δ=1.2-1.8: (6H, $-CH_2CH_2CH_2CH_2NH_2$).

Synthesis of $PLys_{100}$-NHS-$mPEG_{77}$. The synthesis of $PLys_{100}$-NHS-$mPEG_{77}$ was achieved by conjugating $mPEG_{77}$-NHS onto $PLys_{100}$ (Figure S1). Briefly, 100 mg of $PLys_{100}$ was dissolved in PBS buffer (pH 7.4, 10 mM) to reach a concentration of 10 mg/mL, and then 140 mg of $mPEG_{77}$-NHS (five equivalents to amine groups of $PLys_{100}$) was added. After the reaction, unreacted $mPEG_{77}$-NHS was removed by dialysis (MWCO=10000 Da), and $PLys_{100}$-NHS-$mPEG_{77}$ was obtained by lyophilization. The successful synthesis was confirmed using ^1H NMR analysis (Figure S2). ^1H NMR (400 MHz, D_2O, δ ppm): δ=4.2-4.4: (1H, $-NHCHCO-$),δ=3.5-3.7: (4H, $-CH_2CH_2O-$), δ=2.8-3.1: (2H, $-CH_2NH_2$), δ=1.2-1.8: (6H, $-CH_2CH_2CH_2CH_2NH_2$).

Transcription and purification of single-guide RNA (sgRNA). DNA templates encoding a T7 promoter followed by the sgRNA-specific target sequence were synthesized by GenePharma (Suzhou, China). All sgRNAs was transcribed *in vitro* with AmpliScribe™ T7-Flash™ Transcription Kit (Epicentre) according to manufacturer's instructions. *In vitro* transcribed sgRNA was extracted with citrate-saturated phenol:chloroform:isoamyl alcohol (25:24:1, v/v/v), purified with RNase-free DNase, precipitated with 2-propanol, and then re-dissolved in nuclease-free water. The concentration of sgRNA was determined using a Nanodrop 2000 Spectrophotometer (Thermo Fisher Scientific) and the final sgRNA products were stored at -80°C for the subsequent experiments. The target sequences of sgRNAs are shown below: sgEGFP：CAAGTTCAGCGTGTCCGGCG; sgSTAT3: CAACCACCCCACAGCAGCCG; sgRUNX1: GGATGTTCCAGATGGCACTC.

Preparation of nanoRNP and NR-nanoRNP. The nanoRNP and NR-nanoRNP were prepared by mixing the solution of RNP with $PLys_{100}$-CA-$mPEG_{77}$ solution and $PLys_{100}$-NHS-$mPEG_{77}$ solution, respectively. Briefly, Cas9 nuclease (0.1 mL, 2 mg/mL in water) and sgRNA (0.1 mL, 400 μg/mL in water) were mixed gently and incubated for 15 min to form the RNP. To prepare nanoRNP, 0.1 mL of $PLys_{100}$-CA-$mPEG_{77}$ solution (0.64 mg/mL) was added into the solution of RNP (0.1 mL) and incubated for 15 min at room temperature. The preparation of NR-nanoRNP was achieved in a similar method by employing $PLys_{100}$-NHS-$mPEG_{77}$ (0.1 mL, 0.64 mg/mL) instead of $PLys_{100}$-CA-$mPEG_{77}$. In addition, 0.1 mL of $PLys_{100}$ solution (268 μg/mL) was added into the solution of RNP (0.1 mL) and incubated for 15 min at room temperature to form $PLys_{100}$/RNP.

DLS and TEM analysis of nanoRNP and NR-nanoRNP. The average size and zeta potential of nanoRNP and NR-nanoRNP were determined using dynamic light scatting (DLS) measurements. The DLS measurements were performed on a laser light scattering spectrometer (BI-200SM) equipped with a digital correlator (BI-9000AT) at 636 nm at 37°C.

The morphology of nanoRNP and NR-nanoRNP were observed by using transmission electron microscopy (TEM, FEI Talos F200C electron microscope). For the preparation of TEM samples, nanoRNP and NR-nanoRNP were prepared as the solutions with pH 7.4 and the concentration of Cas9 nuclease at 10 μg/mL. TEM samples were prepared by drop-coating of 2 μL nanoRNP and NR-nanoRNP onto carbon-coated copper grids (Beijing Zhongjingkeyi Technology Co., Ltd, China). Droplets of samples were contacted with the grids for 5~10 minutes, then excess amount of samples was removed. The grid was then rinsed and stained with 1% phosphotungstic acid (5~10 μL) for 180 seconds.

Evaluation of the stability of $PLys_{100}$/RNP, nanoRNP, and NR-nanoRNP. The stability of $PLys_{100}$/RNP, nanoRNP, and NR-nanoRNP was analysed using the following method. Briefly, we dissolved the $PLys_{100}$/RNP**,** nanoRNP, and NR-nanoRNP in mouse serum at 37°C, and the size of nanoRNP was characterized at various incubation times using DLS measurements. To evaluate the sgRNA integrity after incubation in mice serum, nanoRNP-STAT3 and NR-nanoRNP-STAT3 pre-cultured with mouse serum were further treated with heparin. Agarose gel was used to detect the sgRNA integrity, and free sgRNA was set as control.

Cell culture. U87MG cells were maintained in DMEM supplemented with 10% (v/v) heat-inactivated fetal bovine serum (FBS), 100 units mL^{-1} penicillin, and 100 μg mL^{-1} streptomycin. All cell cultures were maintained in 5% CO_2 humidified environment at 37°C.

Analyses of cellular uptake. Cellular uptake of nanoRNP was studied using confocal laser scanning microscope (CLSM, Olympus, FV1000) and flow cytometry (Guava, easyCyte 8HT). Briefly, U87MG cells were seeded at a density of 1×10^4 cells per well in a 35 mm confocal dish (Φ =15 mm) and incubated overnight for cell attachment. The cells were then exposed to nanoRNP and NR-nanoRNP containing 2.5 μg FITC labeled Cas9 nuclease and 0.5 μg Cy3 labeled sgRNA, and then incubated in complete culture medium at different pH (pH 7.4 and pH 6.5, respectively) for 2 h. After the incubation, the cells were rinsed with ice-cold PBS and fixed with fresh 4% paraformaldehyde for 15 min at room temperature. The cell nucleus were further counterstained with 4, 6-diamino-2-phenyl indole (DAPI) following the manufacturer's instructions. After the staining, the cells were observed using CLSM (Olympus, FV1000). The cellular uptake efficiency of nanoRNP and NR-nanoRNP was also assessed using flow cytometry analysis. Briefly, U87MG cells were seeded into 6-well plates at a density of 1×10^5 cells per well. After the overnight growth, U87MG cells were exposed to various nanoparticles containing 5 μg FITC labeled Cas9 nuclease and 1 μg Cy3 labeled sgRNA, then incubated in complete culture medium at different pH (pH 7.4 and pH 6.5, respectively) for 2 h. After the trypsin digestion and centrifugation, the cells were collected, washed with cold PBS and fixed with fresh 4% paraformaldehyde for the flow cytometry analysis (Guava, easyCyte 8HT). All of these experiments were performed in triplicate.

EGFP disruption study. To study the gene editing capability of nanoRNP in tumor cells, the reporter cell line with a single copy of destabilized EGFP gene integrated into the genome was first constructed by transduced with Lentivirus (GenePharma, Shanghai, China) encoding EGFP (denoted as U87MG-EGFP cell). Briefly, U87MG-EGFP cells were seeded into 24-well plates at 2×10^4 cells per well and incubated overnight in 0.5 mL DMEM with 10% FBS (v/v). Before the transfection, the culture medium was replaced with the fresh one and adjusted to either pH 7.4 or

6.8. 50 μL of nanoRNP and NR-nanoRNP with 2.5 μg Cas9 nuclease and 0.5 μg sgEGFP were added into the cell cultures, respectively. After 4 h incubation, the culture medium was replaced with 0.5 mL fresh medium containing 10% FBS (v/v) for further 5 days incubation. PBS were employed as controls to perform the same studies. At the end of experiment, the cells were collected, washed with cold PBS and fixed with fresh 4% paraformaldehyde for flow cytometry analysis (Guava, 8HT, guava). The EGFP disruption study was also observed using CLSM. Furthermore, western bolt assay was used to confirm the gene disruption of EGFP. Briefly, U87MG-EGFP cells were seeded into 6-well plates at a density of 1×10^5 cells/well and then treated as the previous description. After 5 days incubation, U87MG-EGFP cells were washed with PBS for three times and then solubilized in 1% Nonidet P-40 lysis buffer. Homogenates were clarified by centrifugation at 20000g for 15 min at 4°C, and protein concentrations were determined with a BCA assay kit. Total protein lysates were separated by SDS-PAGE on 10% SDS acrylamide gels, which were then transferred to PVDF membranes (Millipore, USA). The membranes were incubated with primary antibodies against EGFP (1:1000 dilution; Santa Cruz Biotechnology, CA, USA) overnight, followed by incubating with an HRP-conjugated secondary antibody (1:1000 dilution; Zhongshan Bio Corp, Beijing, China) for 1 h. GAPDH (1:1000 dilution; Santa Cruz Biotechnology) was set as a loading control. All of these experiments were performed in triplicate.

***In vitro* T7E1 assay.** After treating with different formulations, genomic DNA was extracted from U87MG cells using genomic DNA extraction kit and transcribed with two pairs of specific PCR primers (sgSTAT3: TGAGGTAGGAGGATCGCTTGG and TTGACATACTTGCCCATGAGGTT; sgRUNX1: GACAGACCGAGTTTCTAGGGATT and CTTGCTATGGTTAGTCTTGTTCCA) near the cleavage sites to obtain substrates. After purifying by DNA purification kit, disruption efficiencies were detected according to the T7

Endonuclease I Kit. The digested DNA was analyzed using 2% agarose gel electrophoresis. Disruption efficiencies were calculated by Image J.

DNA Sequencing. After 3 days transfection, we selected single cell for further incubation by dilution method. When single cells grown into cell populations, the genomic DNA was extracted by Genomic DNA extraction kit (TIANGEN Biotech, Beijin, China). We amplified the targeted region of STAT3 and RUNX1 with PCR using high-fidelity polymerase and purified the PCR product by DNA purification and recovery kit (TIANGEN Biotech, Beijin, China). The sequence was performed in illumina Hiseq 2500 PE250 (China Novogene Bioinformatics Technology Co. Ltd.).

Cellular immunofluorescence. The expression of STAT3, and phosphorylated STAT3 (pSTAT3), RUNX1, and phosphorylated RUNX1 (pRUNX1) was first studied with cellular immunofluorescence. Briefly, U87MG cells were seeded at a density of 1×10^4 cells per well in a 35 mm confocal dish (Φ =15 mm) and incubated overnight for cell attachment. Before the transfection, the culture medium was replaced with the fresh one and adjusted to either pH 7.4 or 6.8. 50 μL of nanoRNP and NR-nanoRNP with 2.5 μg Cas9 nuclease and 0.5 μg sgSTAT3 (or sgRUNX1) were added into the cell cultures, respectively. After 4 h incubation, the culture medium was replaced with 0.5 mL fresh medium containing 10% FBS (v/v) for further 72 h incubation. After the incubation, the cells were rinsed with ice-cold PBS and fixed with fresh 4% paraformaldehyde for 15 min at room temperature. The fixed cells were washed with PBS containing 0.5% Triton X-100 for 1 h and incubated with primary antibodies against STAT3, pSTAT3 or RUNX1, pRUNX1 (1:1000 dilution; Santa Cruz Biotechnology, CA, USA) overnight, followed by incubating with an fluorescent probe-conjugated secondary antibody for 1 h. Cell

nucleus were further counterstained with DAPI following the manufacturer's instructions. All the cells were observed using a CLSM (Olympus, FV1000).

Western blotting analysis. Western bolt assay was employed to measure the protein expression levels of STAT3, pSTAT3, RUNX1, and pRUNX1. Briefly, U87MG cells were seeded into 6-well plates at a density of 1×10^5 cells/well and then treated as the previous description. After the transfection, each group of cells was washed with PBS for three times and then solubilized in 1% Nonidet P-40 lysis buffer. Homogenates were clarified by centrifugation at 20000g for 15 min at 4°C, and protein concentrations were determined with a BCA assay kit. Total protein lysates were separated by SDS-PAGE on 10% SDS acrylamide gels, which was then transferred to PVDF membranes (Millipore, USA). The membranes were incubated with primary antibodies against STAT3, pSTAT3 and RUNX1, pRUNX1 (1:1000 dilution; Santa Cruz Biotechnology, CA, USA) overnight, followed by incubating with an HRP-conjugated secondary antibody (1:1000 dilution; Zhongshan Bio Corp, Beijing, China) for 1 h. GAPDH (1:1000 dilution; Santa Cruz Biotechnology) was set as a loading control.

***In vitro* cytotoxicity analysis.** The *in vitro* anti-tumor effect of nanoRNP-STAT3 and nanoRNP-RUNX1 were also evaluated by CCK-8 viability assay in a similar method. Briefly, U87MG cells were seeded into 96-well plates at a density of 5×10^3 cells/well and incubated overnight in DMEM with 10% FBS (v/v). The cultures were adjusted to either pH 7.4 or 6.8, and then added 10 μL of naoRNP-STAT3, nanoRNP-RUNX1, respectively (400 ng Cas9 nuclease/well). Free RNP, nanoRNP-NC, NR-nanoRNP-STAT3, and NR-nanoRNP-RUNX1 were used as control. After 4 h incubation, the culture medium was refreshed and further incubated for 72 h. After the incubation, the cells were rinsed using PBS, CCK-8 was mixed with DMEM at a volume ratio of 1/9 (freshly

prepared) to achieve the CCK-8 working solution. After the incubation, the cells were rinsed using PBS buffer, followed by the addition of 100 μL CCK-8 working solution mixture and another 2 h of incubation. Quantification of the cell viability was achieved by measuring the absorbance with Tecan's Infinite M200 microplate reader (λ= 450 nm). The cell viability was calculated by referring to that of the cells without any treatment.

Establishment of tumor heterogeneity model. The $U87MG_{LV\text{-}STAT3}$-mcherry and $U87MG_{LV\text{-}RUNX1}$-GFP cells were obtained by transduced with lentiviruses silencing STAT3 and RUNX1 (GenePharma, Shanghai, China), respectively. After treated with lentiviruses, puromycin was used to further screen cells with higher transfection efficiency. To determine the knockdown of RUNX1 and STAT3 treated with lentiviruses, the target proteins and mRNAs of $U87MG_{LV\text{-}STAT3}$-mcherry and $U87MG_{LV\text{-}RUNX1}$-GFP cells were collected for western bolt and qRT-PCR analysis. Briefly, $U87MG_{LV\text{-}STAT3}$-mcherry and $U87MG_{LV\text{-}RUNX1}$-GFP cells were seeded into 6-well plates at a density of 5×10^5 cells/well and incubated overnight in DMEM with 10% FBS (v/v). After 24 h incubation, the total RNA was extracted from the cells using TRIzol reagent (Invitrogen, USA) according to the manufacturer's instructions. A stem-loop–specific primer (GenePharma, Shanghai, China) was used to measure the expression levels of mSTAT3 and mRUNX1. Expression of U6 was used as an endogenous control. The mRNA was converted to cDNA using the PrimeScript RT reagent kit (TaKaRa, Tokyo, Japan) according to the manufacturer's protocol. cDNAs were quantified by SYBR PremixExTaq (TaKaRa, Japan) by DNA Engine Opticon 2 Two-Color Real-Time PCR Detection System (Bio-Rad, USA). Fold changes for the expression levels of mRNAs (STAT3 and RUNX1) were calculated using the comparative cycle threshold (CT) method ($2^{-\Delta\Delta CT}$). Finally, heterogeneous tumor model was constructed by co-cultivating $U87MG_{LV\text{-}STAT3}$-mcherry and $U87MG_{LV\text{-}RUNX1}$-GFP cells (Quantity ratio=1:1).

Gene disruption and anti-tumor effect of nanoRNP in heterogeneous tumor model *in vitro*. Western bolt was employed to detect the gene editing efficiency in heterogeneous tumor model. Briefly, $U87MG_{LV\text{-}STAT3}$-mcherry and $U87MG_{LV\text{-}RUNX1}$-GFP cells were seeded into 6-well plates at a density of 1×10^5 cells/well (quantity ratio=1:1) and co-incubated overnight in DMEM with 10% FBS (v/v). The cultures were adjusted to either pH 7.4 or 6.8, and then added 100 μL of nanoRNP-STAT3, nanoRNP-RUNX1, and nanoRNP-STAT3+RUNX1 respectively (5 μg Cas9 nuclease/well). After 4 h incubation, the culture medium was refreshed and further incubated for 72 h. After the transfection, each group of cells was washed with PBS for three times and then solubilized in 1% Nonidet P-40 lysis buffer. Homogenates were clarified by centrifugation at 20000g for 15 min at 4°C, and protein concentrations were determined with a BCA assay kit. Total protein lysates were separated by SDS-PAGE on 10% SDS acrylamide gels, which was then transferred to PVDF membranes (Millipore, USA). The membranes were incubated with primary antibodies against STAT3, pSTAT3, RUNX1 and pRUNX1 (1:1000 dilution; Santa Cruz Biotechnology, Santa Cruz, CA, USA) overnight, followed by incubating with an HRP-conjugated secondary antibody (1:1000 dilution; Zhongshan Bio Corp, Beijing, China) for 1 h. GAPDH (1:1000 dilution; Santa Cruz Biotechnology) was set as a loading control.

The *in vitro* anti-tumor effect of nanoRNP-RUNX1+STAT3 was evaluated in heterogeneous tumor model using CCK-8 viability assay in a similar method. Briefly, $U87MG_{LV\text{-}STAT3}$-mcherry and $U87MG_{LV\text{-}RUNX1}$-GFP cells were seeded into 96-well plates at a density of 5×10^3 cells/well (quantity ratio=1:1) and co-incubated overnight in DMEM with 10% FBS (v/v). The cultures were adjusted to either pH 7.4 or 6.8, and then added 10 μL of nanoRNP-STAT3, nanoRNP-RUNX1, and nanoRNP-STAT3+RUNX1, respectively (400 ng Cas9 nuclease/well). After 4 h incubation, the culture medium was refreshed and further incubated for 72 h. After the incubation, the cells

were rinsed using PBS, and the viability was accessed using CCK-8 assay kit. Furthermore, the *in vitro* anti-tumor effect of nanoRNP-RUNX1+STAT3 in heterogeneous tumor model were also directly observed by fluorescence microscope (CX41, Olympus). After 3 days transfection, the *in vitro* anti-tumor effect of nanoRNP-RUNX1+STAT3 was also stained with DAPI and Annexin V-Cy5, and then detected with flow cytometry (Guava, 8HT, guava) .

***In vivo* distribution of nanoRNP.** To investigate the tumor accumulating ability of nanoRNP, female BALB/c nude mice at 4-week old were purchased from the animal center of the Cancer Institute of Chinese Academy of Medical Science, and were bred at Compare Medicine Center, Tianjin Medical University. All experimental protocols were conducted within Tianjin Medical University guidelines for animal research and were approved by Institutional Animal Care and Use Committee. The tumor-bearing mice were established by subcutaneous injection of U87MG cells (1×10^7 for each mouse) in the mammary fat pad. The mice were randomly divided into five groups. When the tumor volume was about 500 mm^3, the mice were intravenous injected with 100 μL of PBS, free RNP, $PLys_{100}$/RNP, NR-nanoRNP and nanoRNP containing 10 μg Cy-5.5 labeled Cas9 nuclease. At 2 h, 6 h and 24 h post-injection, the mice were observed and imaged by IVIS Lumina imaged system (Caliper Life Sciences, USA). Then the mice were sacrificed, and the major organs and the tumors were collected for *ex vivo* imaging. The fluorescence images were analyzed using Living Image 3.1 (Caliper Life Sciences). To determine *in vivo* uptake of nanoRNP by tumor cells, the tumors were treated as single cell suspension and analyzed with flow cytometry (Guava, 8HT, guava) at 24 h post-injection.

Immunogenicity evaluations assessed with inflammatory cytokine secretion. 12 Male KunMing mice of 8-10-week-old were divided into 2 groups and injected with 100 μL of PBS and

nanoRNP-STAT3 containing 10 μg Cas9 nuclease per mouse via tail vein three times in two weeks. The blood samples were collected from the mice with coagulant tube, which allows the blood to coagulate naturally. The blood samples were then centrifuged at 2000 rpm for 10 minutes, and the levels of IgG, IgE, IgM, IL-6, IFN-γ, TNF-α and NF-kB in the supernatant was assessed using a mouse IgG, IgE, IgM, IL-6, IFN-γ, TNF-α and NF-kB ELISA kits following the protocol provided by the manufacture. The measurements were performed on a Tecan's Infinite M200 microplate reader.

Tumor Growth Suppression with nanoRNP-STAT3. To study the feasibility of nanoRNP for CRISPR/Cas9-based tumor gene therapy *in vivo*, the tumor-bearing mice with U87MG xenograft was established as described above. When the tumor volume was around 50 mm^3 at 14 days after cell implantation, the mice were randomly divided into six groups (six mice per group) and intravenously injected with 100 μL of PBS, nanoRNP-NC, free RNP-STAT3, $PLys_{100}$/RNP-STAT3, NR-nanoRNP-STAT3 and nanoRNP-STAT3 containing 10 μg Cas9 nuclease per mouse every three days. Tumor growth was monitored by measuring the perpendicular diameter of the tumor using calipers. The estimated volume was calculated according to the formula: tumor volume (cm^3) = 0.5 × length × $width^2$.

Western bolt analysis of protein from tumors and normal organs. For analysis the gene disruption *in vivo*, the mice administrated with different formations were sacrificed, and their tumors and other organs (e.g., heart, liver, spleen, lung, kidney) were collected, freezed with liquid nitrogen and grind. The protein was collected and analyzed by western bolt as describe above.

Immunohistochemistry, immunofluorescence and H&E analysis. For immunohistochemistry analysis and H&E staining, tumor tissues were immersed in 4% paraformaldehyde at 4°C for 24

h, followed by incubating with different concentrations of alcohol to remove moisture. The tissues were then embedded in paraffin. 8 μm of tissue slices were prepared with cryosections and air dried for 4 h min at 60°C for immunohistochemistry analysis. For STAT3 and pSTAT3 analyzing, the fixed tumor sections were incubated with primary antibodies (1:200 dilutions) overnight at 4°C, followed by incubating with biotin-labeled secondary antibody (1:200 dilutions) for 1 h at 37°C. The sections were then incubated with ABC-peroxidase and diaminobenzidine (DAB), counterstained with hematoxylin, and visualized using light microscope (CX41, Olympus). For immunofluorescencean staining, tumor tissues were immersed in 4% paraformaldehyde at 4°C for 24 h, followed by incubating with 30% sucrose solution (w/w) overnight. The tissues were then embedded in OCT (optimal cutting temperature compound) before storing at -80°C. 8 μm of tissue slices were prepared with cryosections and air dried for 30 min at 25°C for immunofluorescencean analysis. For the deoxynucleotidyl transferase dUTP nick end labeling (TUNEL) apoptosis studying, the fixed tumor sections were stained using TUNEL Apoptosis Assay Kit according to the manufacturer's protocol. DAPI was used for nuclear counterstaining. For Ki-67 studying, the fixed tumor sections were incubated with primary antibodies against Ki-67 (1:100 dilutions) overnight at 4°C, followed by incubating with fluorescently labeled-secondary antibody (1:200 dilutions) for 1 h at 37°C. DAPI was used for nuclear counterstaining. All immunofluorescencean slices were were observed using a CLSM (Olympus, FV1000).

Overcome tumor heterogeneity with nanoRNP-STAT3+RUNX1. To investigate tumor growth inhibition with nanoRNP-STAT3+RUNX1 in heterogeneous tumor, female BALB/c nude mice at 4-week old were purchased from the animal center of the Cancer Institute of Chinese Academy of Medical Science, and were bred at Compare Medicine Center, Tianjin Medical University. All experimental protocols were conducted within Tianjin Medical University guidelines for animal

research and were approved by Institutional Animal Care and Use Committee. The tumor-bearing mice were established by subcutaneous injection of $U87MG_{LV\text{-}STAT3}$-mcherry and $U87MG_{LV\text{-}RUNX1}$-GFP cells (1×10^7 for each mouse, quantity ratio=1:1) in the mammary fat pad. When the tumor volume was around 40 mm^3 at 14 days after cell implantation, the mice were randomly divided into four groups (six mice per group) and intravenously injected with 100 μL of PBS, nanoRNP-STAT3, nanoRNP-RUNX1, nanoRNP-STAT3+RUNX1 containing 10 μg Cas9 nuclease per mouse every five days. Tumor growth was monitored by measuring the perpendicular diameter of the tumor using calipers. The estimated volume was calculated according to the formula: tumor volume (cm^3) = 0.5 × length × $width^2$. For analysis the gene disruption *in vivo*, the mice administrated with different formations were sacrificed, and their tumors and other organs (e.g., heart, liver, spleen, lung, kidney) were collected, freezed with liquid nitrogen and grind. The protein was collected and analyzed by western bolt as describe above. For mmunohistochemistry, immunofluorescencean and H&E analysis, the tumors and normal organs (e.g., heart, liver, spleen, lung, kidney) from the mice treated with different formations were collected and studied as describe above.

Statistical Analysis. Statistical comparisons were achieved using one-way ANOVA with Dunnett post-test with GraphPad Prism 5.0.

REFERENCE

(1) Liu, Q.; Zhao, K.; Wang, C.; Zhang, Z.; Zheng, C.; Zhao, Y.; Zheng, Y.; Liu, C.; An, Y.; Shi, L.; Kang, C.; Liu, Y. *Adv. Sci.* **2019**, *6*, 1801423.
(2) Sun, C.-Y.; Shen, S.; Xu, C. F.; Li, H.-J.; Liu, Y.; Cao, Z.-T.; Yang, X.-Z.; Xia, J. X.; Wang, J. *J. Am. Chem. Soc.* **2015**, *137*, 15217-15224.
(3) Lee, Y.; Miyata, K.; Oba, M., Ishii, T., Fukushima, S.; Han, M.; Koyama, H.; Nishiyama, N.; Kataoka, K. *Angew. Chem. Int. Ed.* **2008**, *47*, 5163-5166.

Supplementary figures

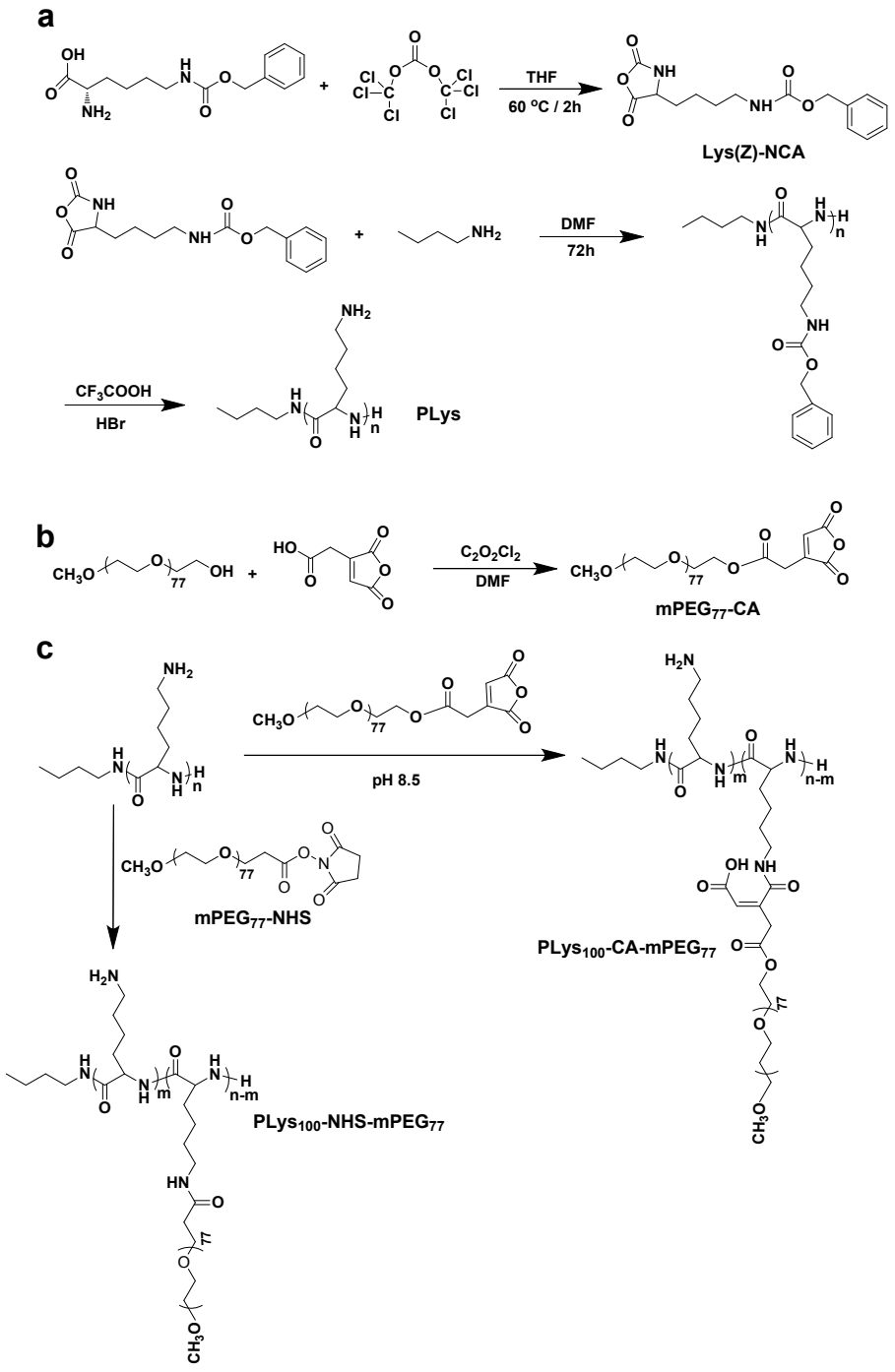

Figure S1. Synthesis routes of $PLys_{100}$ (a), $mPEG_{77}$-CA (b), $PLys_{100}$-CA-$mPEG_{77}$ and $PLys_{100}$-NHS-$mPEG_{77}$ (c).

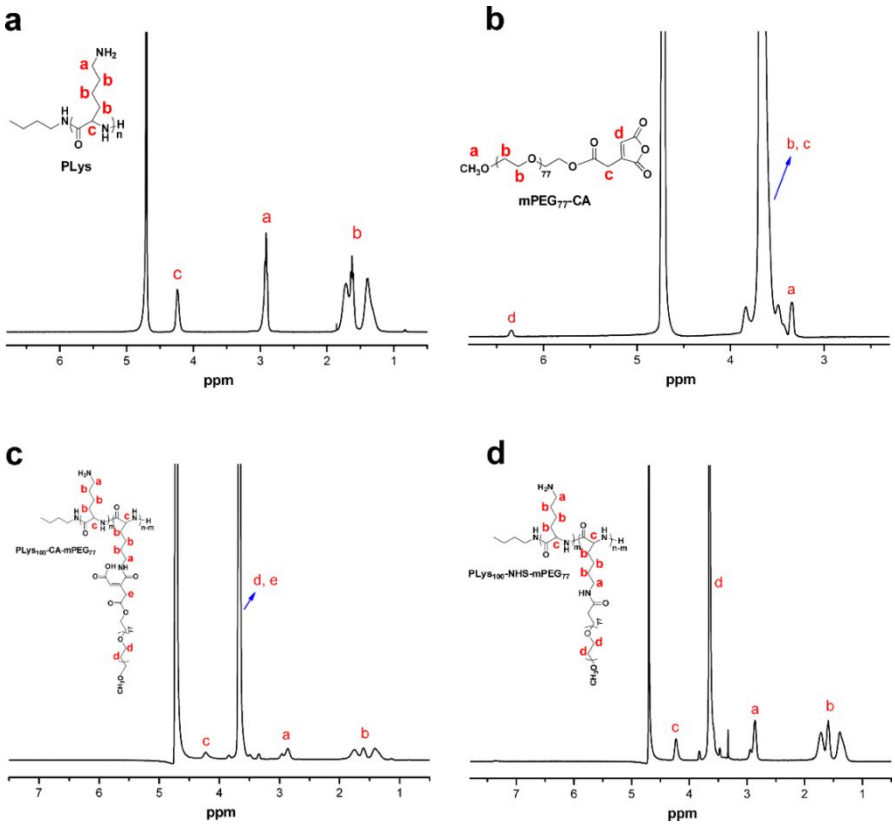

Figure S2. ^{1}H NMR spectra of $PLys_{100}$ (a), $mPEG_{77}$-CA (b), $PLys_{100}$-CA-$mPEG_{77}$ (c) and $PLys_{100}$-NHS-$mPEG_{77}$ (d) in D_2O.

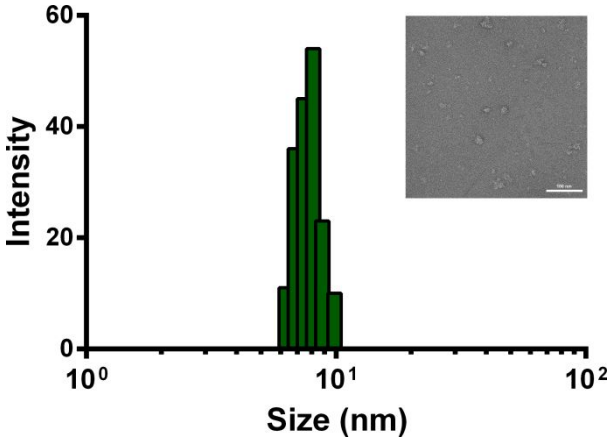

Figure S3. DLS and TEM measurements of RNP**.** The scale bars are 100 nm.

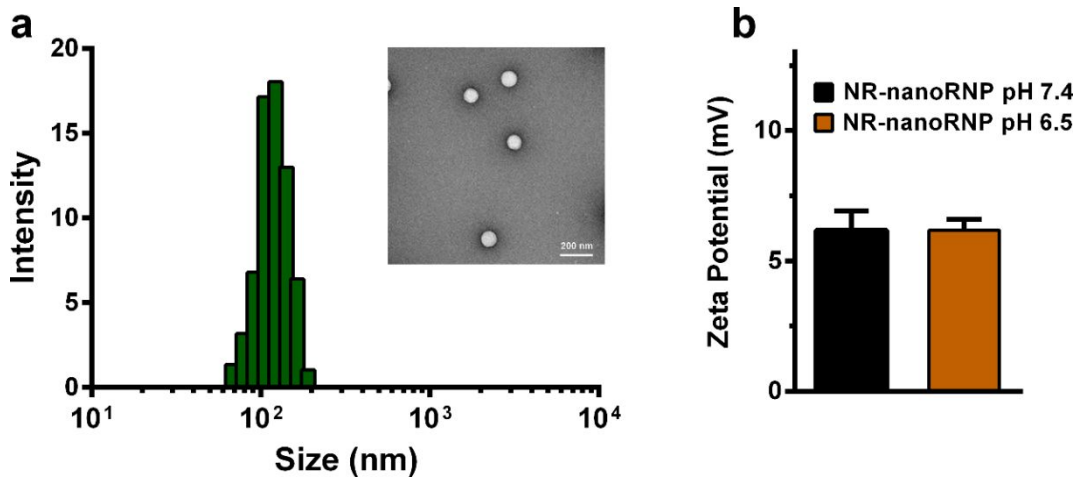

Figure S4. a) DLS and TEM measurements of NR-nanoRNP**.** The scale bars are 200 nm. b) Zeta potential of NR-nanoRNP at pH 7.4 and 6.5. Data represent mean ± s.d. from three independent experiments (n = 3).

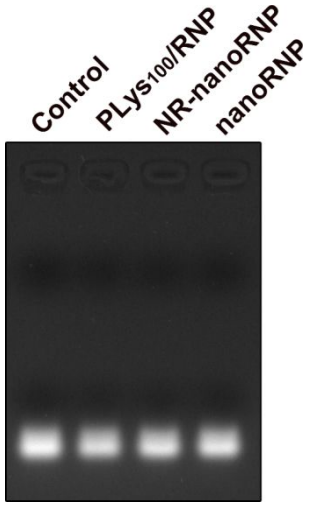

Figure S5. Agarose gel analysis of sgRNA integrity after incubation in mice serum.

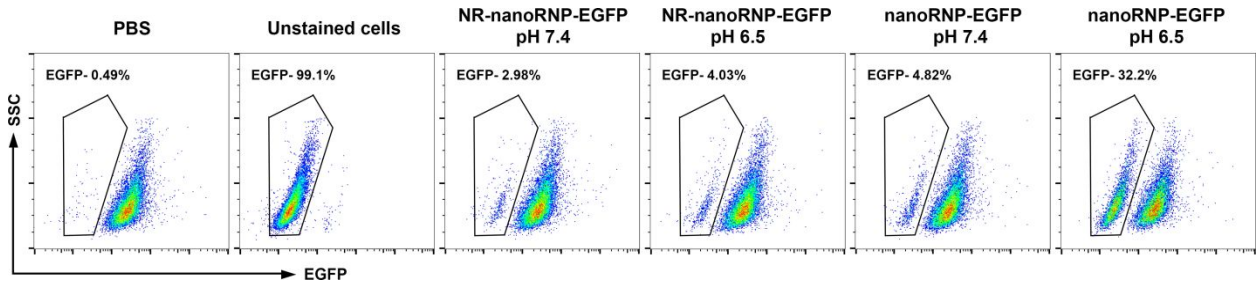

Figure S6. Flow cytometry analysis of EGFP expression in U87MG cells after treated with nanoRNP-EGFP and NR-nanoRNP-EGFP at different pHs.

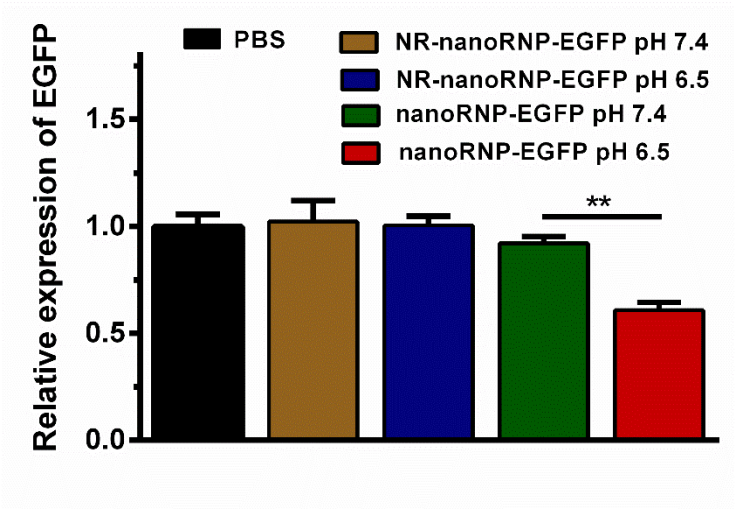

Figure S7. Quantification of EGFP expression in western bolt analysis. Data represent mean ± s.d.. Data represent mean ± s.d. from three independent experiments (n = 3) and the significance levels are **P<0.01.

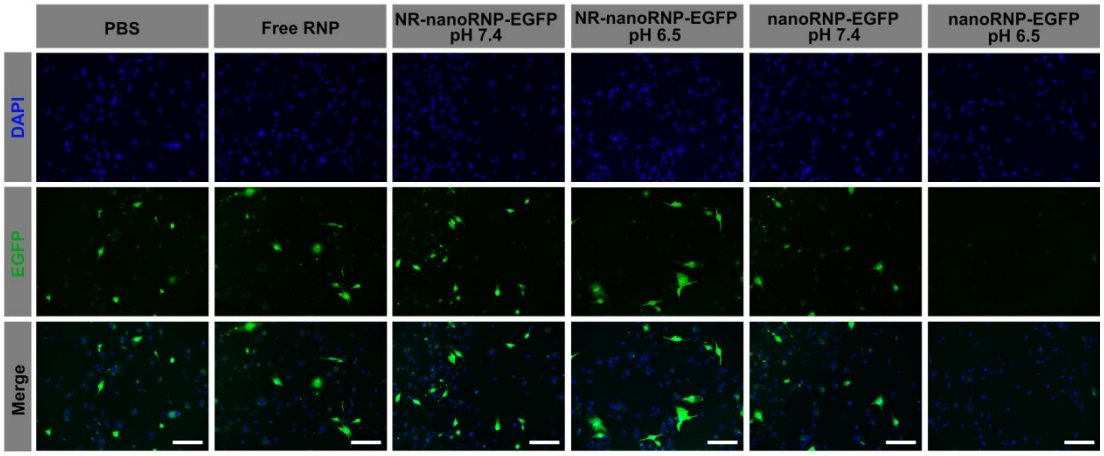

Figure S8. Fluorescence microscopy images of EGFP disruption treated with different formulations in U87MG-EGFP cells. Green, EGFP; blue, nuclei stained with DAPI. Scale bars are 100 μm.

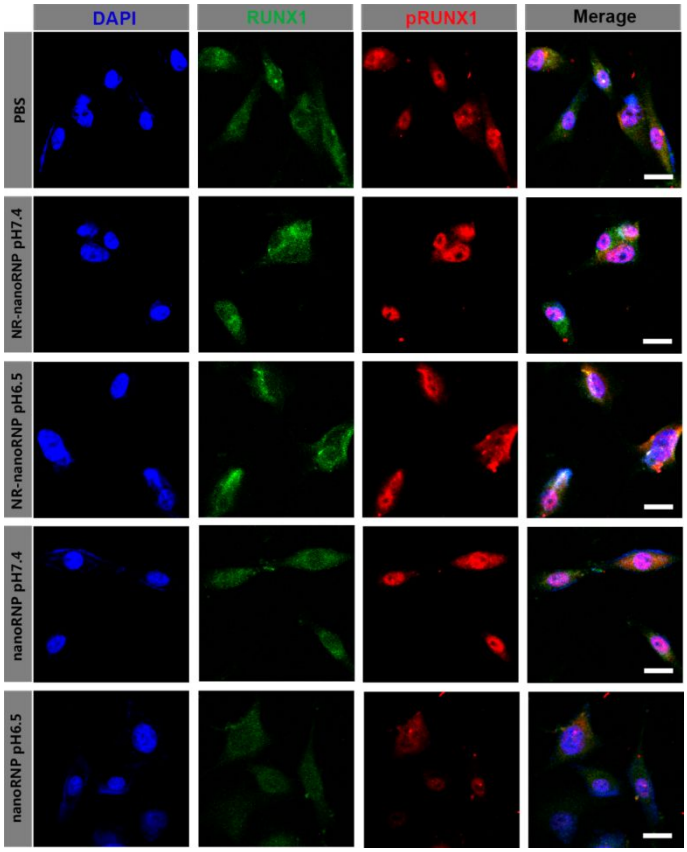

Figure S9. Immunofluorescence analyses of the expression of RUNX1 and pRUNX1 treated with NR-nanoRNP-RUNX1 and nanoRNP-RUNX1 at different pHs. Cell nuclei are stained with DAPI (blue), RUNX1 and pRUNX1 are stained with AlexaFluor 488 (green) and AlexaFluor 594 (red), respectively. The scale bars are 20 μm.

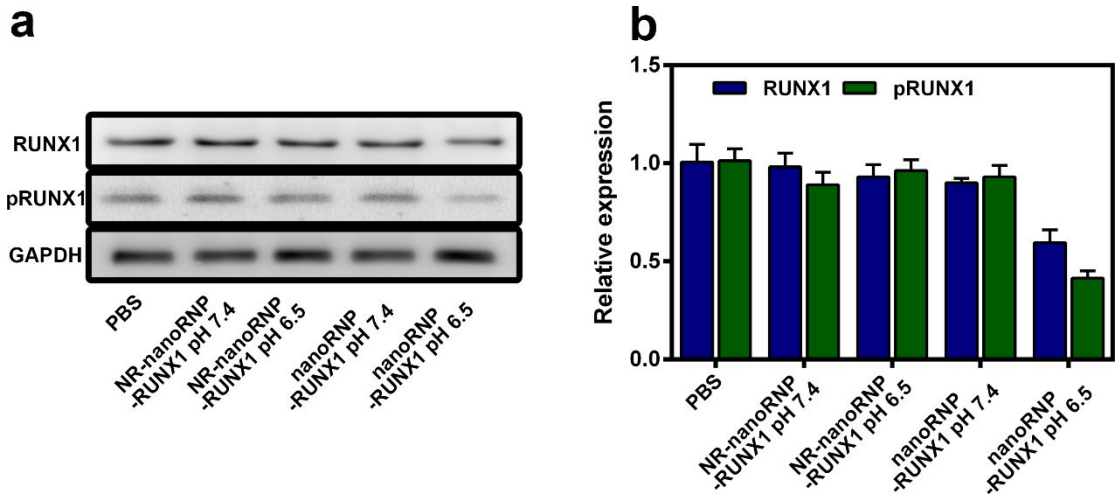

Figure S10. a) Western bolt analyses of the expression of RUNX1 and pRUNX1 treated with NR-nanoRNP-RUNX1 and nanoRNP-RUNX1 at different pHs. GAPDH was used as a loading control. b) Quantitative analysis of RUNX1 and pRUNX1 expression in western bolt assay. Data represent mean ± s.d. from three independent experiments (n = 3).

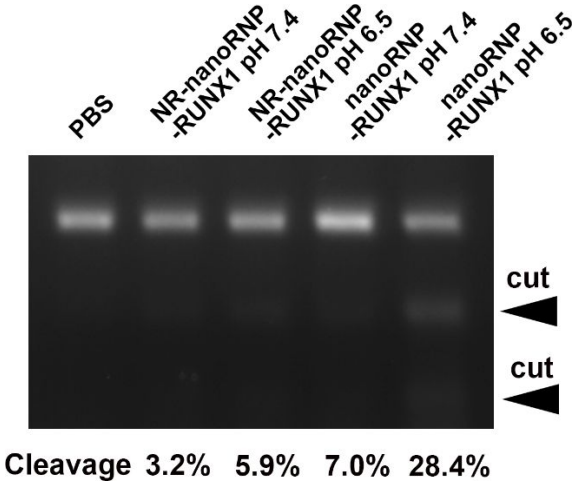

Figure S11. T7E1 assay of U87MG cells treated with NR-nanoRNP-RUNX1 and nanoRNP-RUNX1 at different pHs.

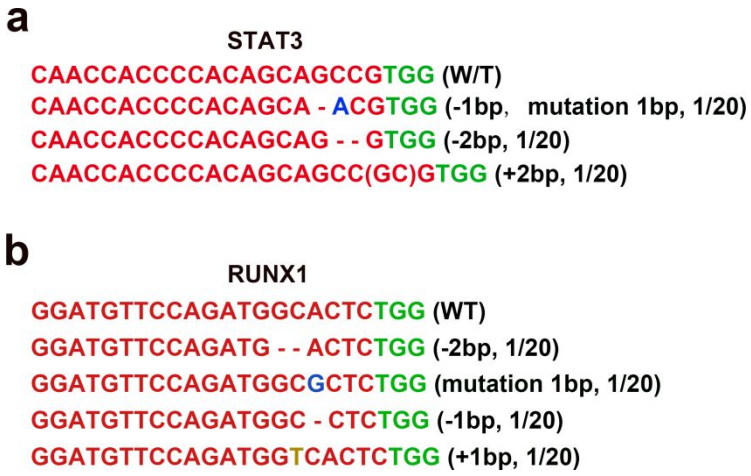

Figure S12. Representative DNA sequences of STAT3 (a) and RUNX1 (b) detected in mutant colonies treated with nanoRNP-STAT3 and nanoRNP-RUNX1.

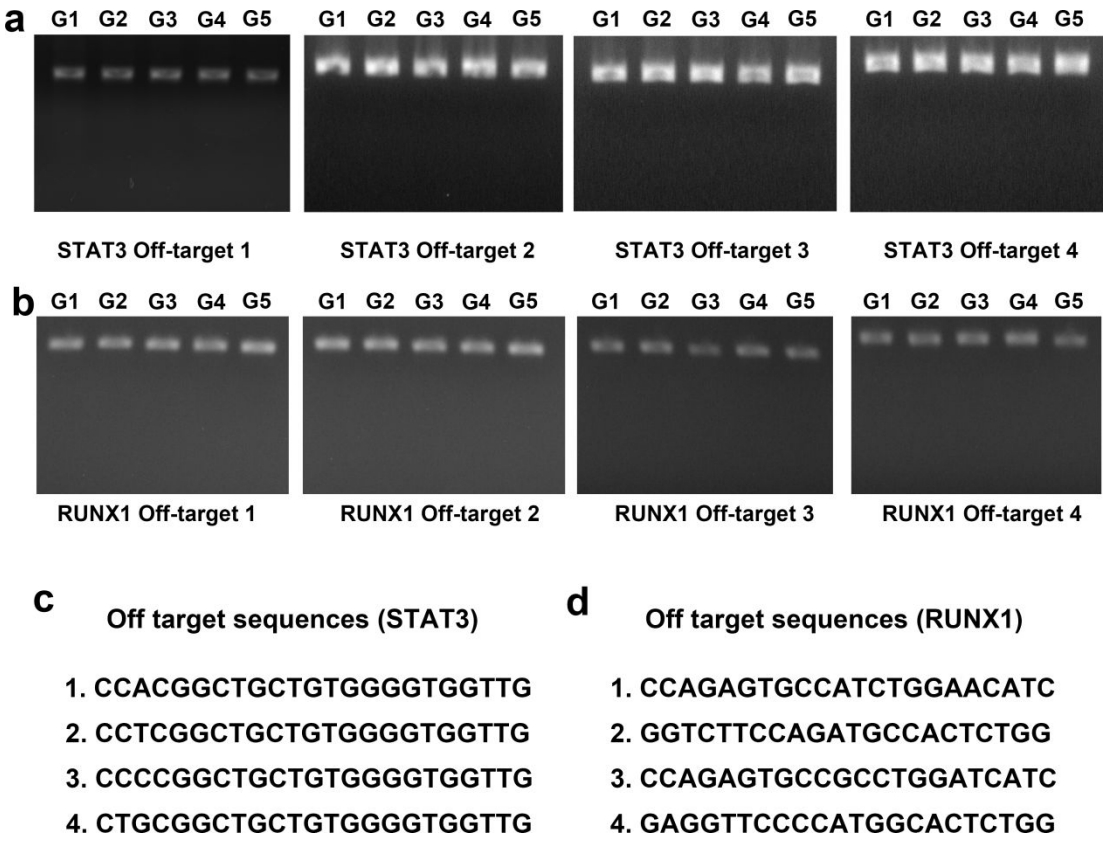

Figure S13. a, b) T7E1 analysis of the potential off-target effect in U87MG cells treated with nanoRNP-STAT3 (a) or nanoRNP-RUNX1 (b). (G1) PBS, (G2) free RNP, (G3) $PLys_{100}$/RNP, (G4) NR-nanoRNP, and (G5) nanoRNP. c, d) Potential off-target sequences of STAT3 (c) and RUNX1 (d).

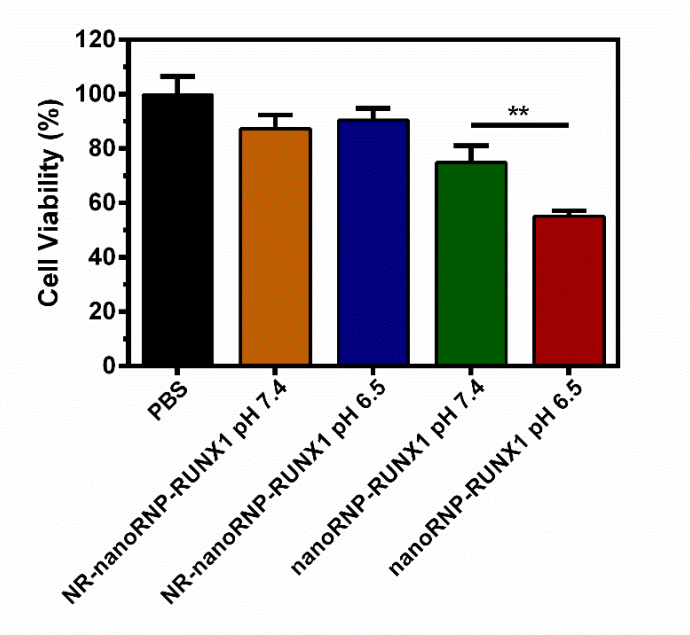

Figure S14. Cell viability of U87MG cells after treating with NR-nanoRNP-RUNX1 and nanoRNP-RUNX1 at pH 7.4 and pH 6.5 for 72 h incubation. Cell viability was assessed using CCK-8 assay. Data represent mean ± s.d. from three independent experiments (n = 3) and the significance levels are **P<0.01.

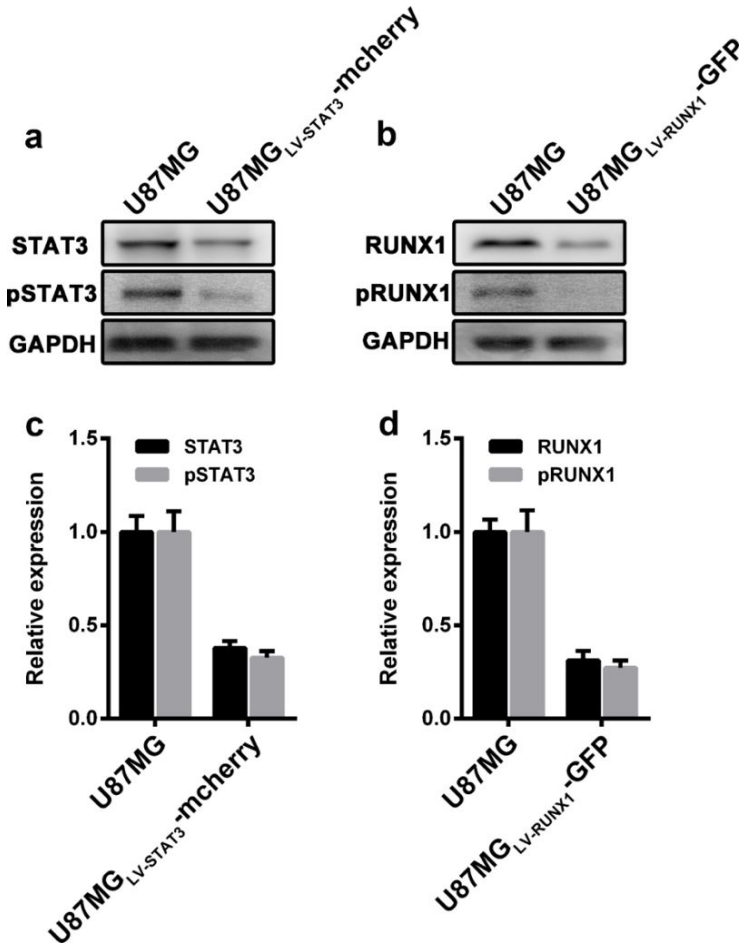

Figure S15. a) Western bolt analyses of the expression of STAT3 and pSTAT3 after transduced with lentivirus silencing STAT3. b) Western bolt analyses of the expression of RUNX1 and pRUNX1 after transduced with lentivirus silencing RUNX1. GAPDH was used as a loading control. c, d) Quantitative analysis of STAT3 and pSTAT3 (c) or RUNX1 and pRUNX1 (d) expression in western bolt assay. Data in (c) and (d) represent mean ± s.d. from three independent experiments (n = 3).

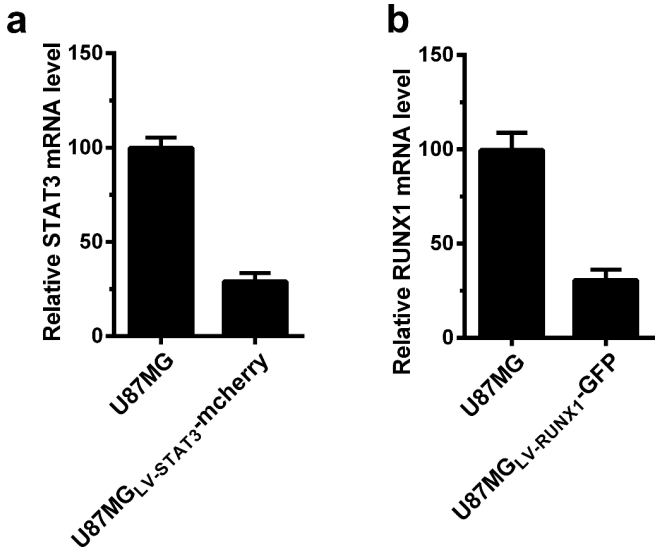

Figure S16. The qRT-PCR analyses of the expression of mRNA (STAT3) (a) and mRNA (RUNX1) (b) in U87MG$_{LV-STAT3}$-mcherry and U87MG$_{LV-RUNX1}$-GFP cells, respectively. Data in (a) and (b) represent mean ± s.d. from three independent experiments (n = 3).

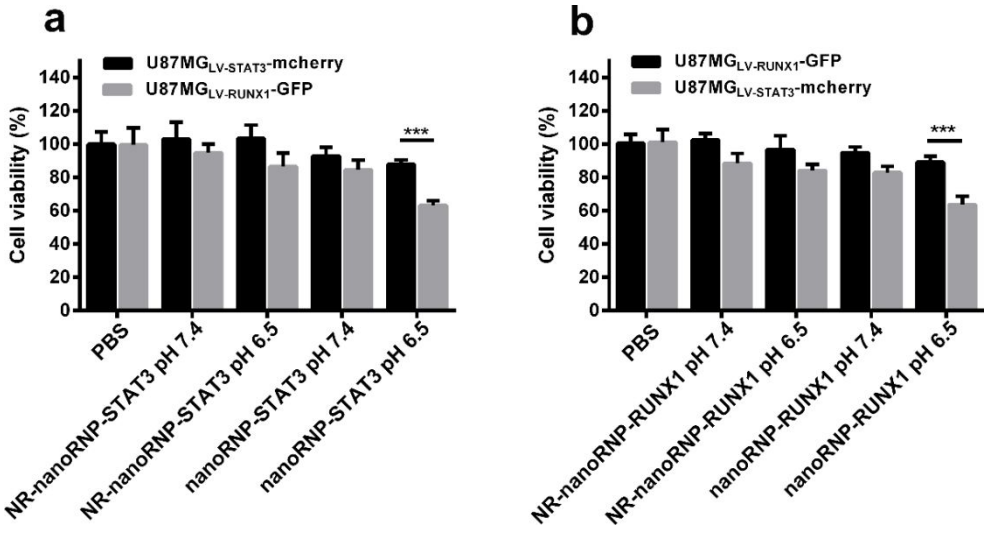

Figure S17. Cell viability of U87MG$_{LV-STAT3}$-mcherry and U87MG$_{LV-RUNX1}$-GFP cells treated with different formations carrying sgSTAT3 (a) and sgRUNX1 (b). Data in (a) and (b) represent

mean ± s.d. from three independent experiments (n = 3) and the significance levels are ***P<0.001.

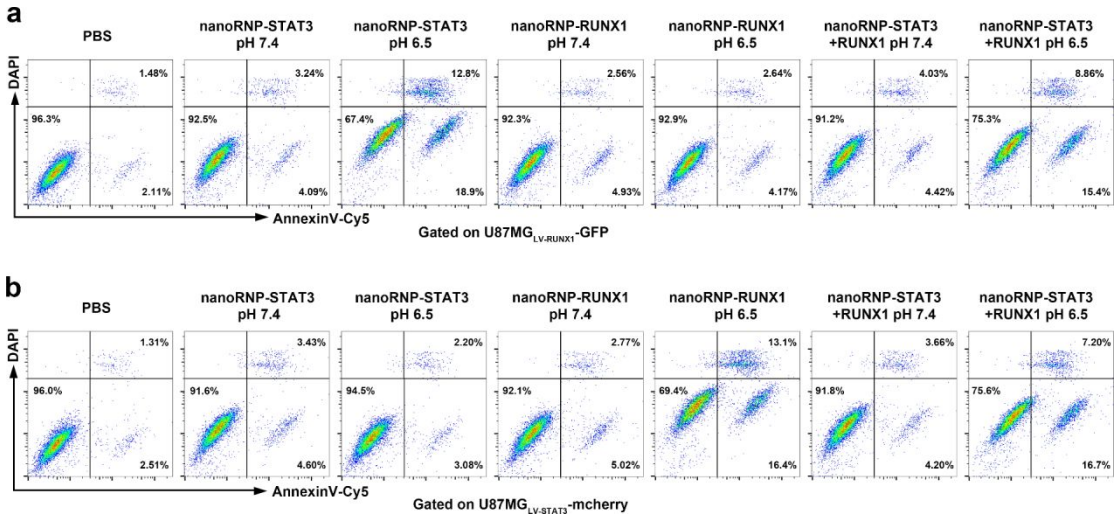

Figure S18. Flow cytometry analysis of the specific cell apoptosis of U87MG$_{LV-RUNX1}$-GFP (a) and U87MG$_{LV-STAT3}$-mcherry (b) in heterogeneous tumor model after treating with different formations.

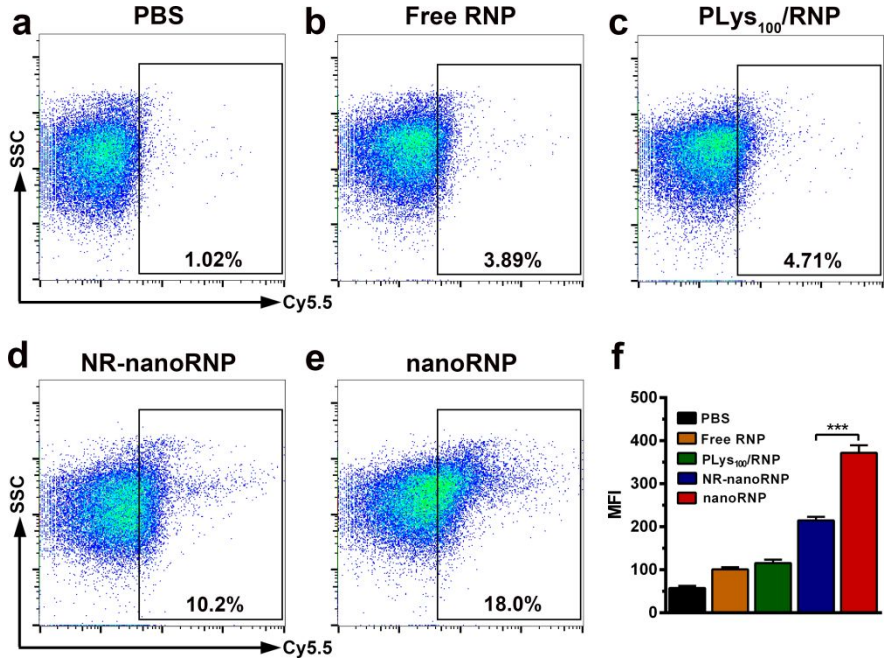

Figure S19. (a-e) Flow cytometry analysis of the tumor cells from the nude mice bearing U87MG tumors at 24 h after intravenous injection of PBS (a), free RNP (b), $PLys_{100}$/RNP (c), NR-nanoRNP (d), and nanoRNP (e). The Cas9 in free RNP, $PLys_{100}$/RNP, NR-nanoRNP and nanoRNP were labeled with Cy5.5. (f) Quantification analysis of the cell uptake *in vivo* shown by mean fluorescence intensity (MFI). Data in (f) represent mean ± s.d. from three independent experiments (n = 3) and the significance levels are ***P<0.001.

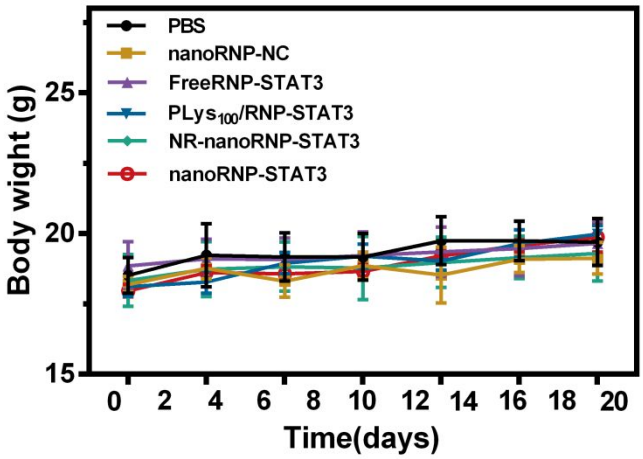

Figure S20. Changes in body weight after treating the mice with different formulations. Data represent mean ± s.d. from six independent experiments (n = 6).

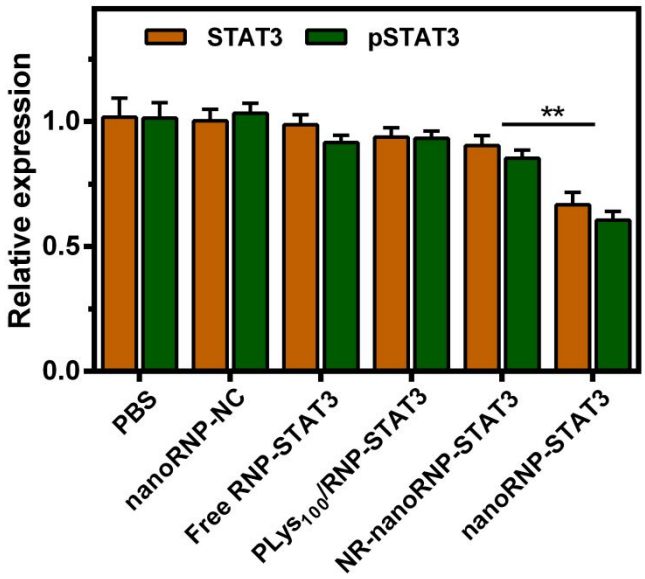

Figure S21. Relative expression levels of STAT3 and pSTAT3 in tumors from the mice treated with different formations. Data represent mean ± s.d. from three independent experiments (n = 3) and the significance levels are **P<0.01.

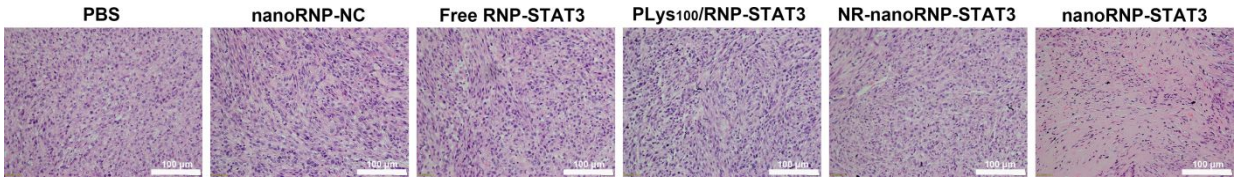

Figure S22. H&E staining analysis of the tumor tissues from the mice in each treatment group.

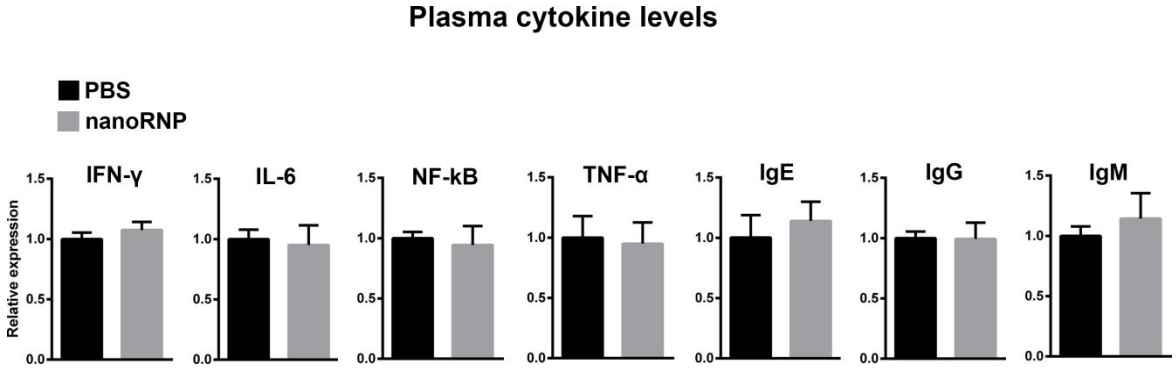

Figure S23. Plasma cytokine levels after the injection of nanoRNP. PBS was used as control. IFN-γ, interferon α; IL-6, interleukin 6; TNF-α, tumor necrosis factor α; NF-kB, nuclear factor kB. Data represent mean ± s.d. from six independent experiments (n = 6).

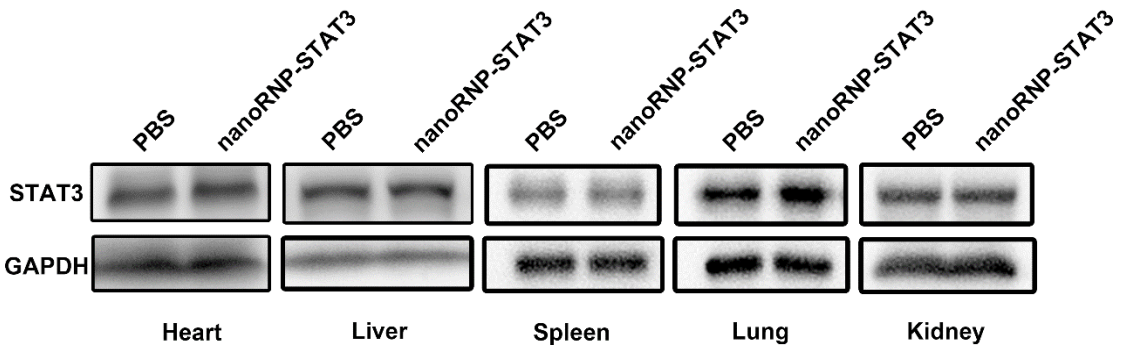

Figure S24. Western bolt analyses of the expression of STAT3 in normal organs (heart, liver, spleen, lung, and kidney) from the mice treated with PBS and nanoRNP-STAT3.

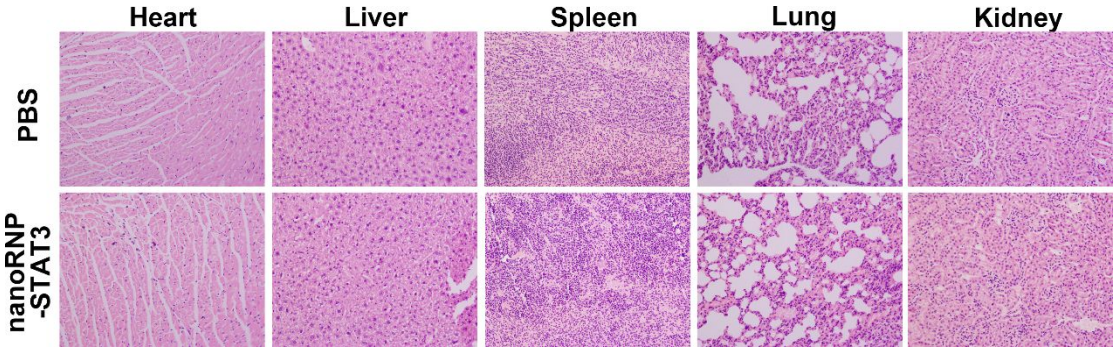

Figure S25. H&E staining analysis of normal organs (heart, liver, spleen, lung, and kidney) tissues from the mice treated with PBS and nanoRNP-STAT3.

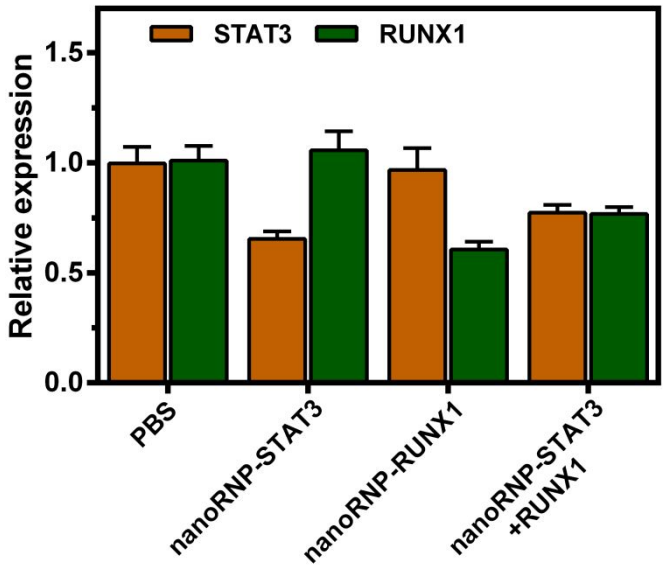

Figure S26. Relative expression levels of STAT3 and RUNX1 in tumors from the mice treated with nanoRNP-STAT3, nanoRNP-RUNX1, and nanoRNP-STAT3+RUNX1. Data represent mean ± s.d. from three independent experiments (n = 3).